Reliability-Based Design Optimization Method of Turbine Disk with Transformed Deterministic Constraints

Dian-Yin Hu[1]; Jun-Jie Yang[2]; Cheng-Wei Fei[3]; Rong-Qiao Wang[4]; and Yat-Sze Choy[5]

[1]*Associate Professor, School of Energy and Power Engineering, Beihang Univ., Collaborative Innovation Center of Advanced Aero-Engine, Beijing Key Laboratory of Aero-Engine Structure and Strength, Xueyuan Rd. No. 37, Haidian District, Beijing 100191, P.R. China.*

[2]*Assistant Professor, School of Aerospace Engineering, Tsinghua Univ., Beijing 10084, P.R. China.*

[3]*Research Fellow, Dept. of Mechanical Engineering, Hong Kong Polytechnic Univ., Kowloon, Hong Kong; Postdoctor Research Fellow, School of Energy and Power Engineering, Beihang Univ., Xueyuan Rd. No. 37, Haidian District, Beijing 100191, P.R. China (corresponding author). E-mail: feicw544@163.com*

[4]*Professor, School of Energy and Power Engineering, Beihang Univ., Collaborative Innovation Center of Advanced Aero-Engine, Beijing Key Laboratory of Aero-Engine Structure and Strength, Xueyuan Rd. No. 37, Haidian District, Beijing 100191, P.R. China.*

[5]*Associate Professor, Dept. of Mechanical Engineering, Hong Kong Polytechnic Univ., Kowloon, Hong Kong.*

Abstract: To improve the computational efficiency of the reliability-based design optimization (RBDO) of a complex structure with nonlinear and implicit limit-state function, the single-loop-single-vector (SLSV)-limit-state factor (LSF) (SLSV-LSF) method was developed by fully considering the advantages of the SLSV approach and the LSF method to transform uncertain constraints into deterministic constraints. The mathematical models of SLSV and LSF were established and the basic RBDO process of the SLSV-LSF method is presented. The shape optimization of an aeroengine turbine disk was completed based on the proposed method. From the reliability sensitivity analysis of the turbine disk, it is revealed that an uncertain constraint of average circumferential stress can be transformed into a deterministic constraint and material density can be regarded as a deterministic variable. Through the min-mass shape design of the turbine disk based on different approaches, it is demonstrated that the developed method maintains high computational speed and efficiency while keeping maintaining computational accuracy, which validates the feasibility and validity of the SLSV-LSF method in the RBDO of aeroengine typical components.

Author keywords: Turbine disk; Reliability-based design optimization; Mean value-based single-loop-single-vector; Limit-state factor; Reliability analysis.

Introduction

Along with the development of aerospace vehicles, the ever- increasing demand for aeroengine components drives designers to continue to strive for better performance, higher reliability, and lower cost and risk. A turbine disk, as one of the typical aeroengine components, endures mechanical and thermal loads under operation conditions, which may induce intensive stresses and dangerous damage (Hu et al. 2011; Fei et al. 2015b). For this reason, the mass of the turbine disk is one of the major factors causing intensive stresses and dangerous damage (Hu and Wang 2008; Hu et al. 2011; Fei et al. 2015b). It is desired to reduce the mass of the tur- bine disk without sacrificing strength or reliability. During turbine disk production and operation, the quantities of dimensions, material properties and loadings, which lead to the change and fluc- tuation of turbine disk performance and mass, have significant dispersibility and are uncertainties, resulting potentially in unantici- pated failure and fault (Fei et al. 2016; Huang et al. 2011). There- fore, it is crucial to consider the uncertainties for the optimization of turbine disk design.

In the traditional design for the uncertainties, constraints im- posed on the design are often reformulated with empirical or other predefined factors instead of the marginal design philosophy, to maintain redundancy of the component. For example,

the stress constraints are often rewritten by multiplying the actual stress with a safety factor (larger than 1) to represent the consideration of all the potential uncertainties (Huang et al. 2011; Yao et al. 2011; Elms 2004). The safety factor is defined mainly based on prior experi- ences and knowledge, such as the U.K. Spey-MK202 engine stress Standard EGD-3 (Ding and Wu 1979). A safety factor that is too large always causes overweight and excessive cost for turbine disk design, whereas a too-small safety factor cannot guarantee the reliability of the system. It is difficult for traditional design ap- proaches to perfectly balance mass (cost) and reliability of a turbine disk by a predefined safety factor because it has frequently proved to be overly conservative (Huang et al. 2011). To address this issue, reliability-based design optimization (RBDO) is proposed to seek a compromise between reliability and cost (Tu and Choi 1999).

The RBDO is formulated as a nested iteration loop problem and widely applied in many fields, such as geological structure (Basha and Babu 2010, 2011), engineering structures (Papadrakakis et al. 2005; Doltsinis and Kang 2004; Kokkolaras et al. 2006), building and environment (Spence and Gioffre 2011; Huang et al. 2012; Mishra et al. 2013), and aerospace engineering (Fei et al. 2014a, 2015a, 2016). Major research efforts are focusing on the efficient formulation and solution techniques of RBDO problems for static and time-varying systems with linear and nonlinear deterministic behavior. However, for the RBDO of a turbine disk, it is a serious problem to overcome computational efficiency because a high computational burden exists, resulting from a large sum of uncertainties and iterates in the nested iteration loop problem. Thus, the computational efficient method is urgently proposed for turbine disk RBDO to reduce the computational cost.

In RBDO methodologies, the reliability index approach (RIA) [also called first-order reliability method (FORM), Liu and Der Liureghian 1991] and performance measure approach (PMA, also known as the fixed-norm approach, Tu and Choi 1999) are two conventional RBDO methods and structured as nested iteration loop problems, which do not satisfy the efficiency requirement of turbine disk RBDO. Recently, various RBDO methods have been developed by transforming reliability constraints into deterministic constraints, which reduce the loop number of reliability analysis (Fei et al. 2014b; Chiralaksanakul and Mahadavan 2005; Liang et al. 2007; Ching and Hsu 2008b, c). Chen et al. (1997) developed a single-loop method called single-vector-single-loop (SLSV) that enables single-loop design optimization by replacing the reliability constraints to equivalent deterministic constraints by using an approximate design point [or most probable point (MPP)] information. Wu et al. (2001) proposed serial single-loop methods called the safety factor approach (SFA), which solve deterministic optimization after alternating the value of constraints or constraints shift by using MPP information obtained from reliability assessment. Yang and Gu (2004, 2005) compared the computational efficiency and the reliability approximation accuracy of the SLSV, SFA, and sequential optimization and reliability assessment (SORA), and Kogiso et al. (2012) specifically investigated the SLSV method for efficient RBDO. The SLSV was reported to be a promising method from the efficiency point of view (Yang and Gu 2004, 2005; Kogiso et al. 2012). However, the RBDO problem of turbine disks obviously involves a high nonlinear and implicit limit-state function. The SLSV method is used to solve the RBDO problem by using FORM where the limit-state function is linear so that the method cannot handle a nonlinear problem (Lee et al. 2008). Besides, it is difficult to obtain the derivatives of the limit-state function of a complex system because the limit-state function is often implicit. The limit-state factor (LSF) method was proposed by integrating limit-state the reliability constraints to deterministic nominal constraints and was validated to be a promising method in processing nonlinear and implicit RBDO problems besides high computational consumption (Chiralaksanakul and Mahadavan 2005; Liang et al. 2007; Ching and Hsu 2008a).

Concentrating on the properties of the limit-state function, this paper presents the SLSV-LSF method to improve the computational efficiency and precision for the RBDO of a turbine disk by transforming uncertainty parameters and constraints into deterministic parameters and constraints. The SLSV-LSF method fully adopts the advantages of the SLSV and LSF approaches.

In the following sections, the method of RBDO for aerospace engineering design is introduced containing RBDO model, SLSV method, LSF approach, and SLSV-LSF method. Next is an explanation of how the RBDO of a turbine disk was implemented to gain low mass and high reliability by this proposed method transforming uncertain constraints of the turbine disk into deterministic constraints based on the LSF approach and SLSV method. The paper ends with some conclusions regarding this study.

RBDO Model

Formulation of RBDO

In this study, the general statement of the RBDO problem in Eq. (1) is given to minimize the objective function subjected to the reliability constraints (Tu and Choi 1999; Yang and Gu 2004, 2005; Kogiso et al. 2012; Lee et al. 2008; Shan and Wang 2008) as follows:

$$\min f(\boldsymbol{d}) \quad \boldsymbol{d} \in R^k$$
$$\text{s.t.} \begin{cases} P[g_i(\boldsymbol{d}, \boldsymbol{X}, \boldsymbol{Z}) < 0] \le P_{F_i}^* \; i = 1, \ldots, n & \boldsymbol{X} \in R^m \\ c_j(\boldsymbol{d}) \le 0 \; j = 1, \ldots, t & \boldsymbol{Z} \in R^q \end{cases} \tag{1}$$

where the probabilistic constraints are described by the limit-state function g_i ($\boldsymbol{d}$, $\boldsymbol{X}$, $\boldsymbol{Z}$), their probability distributions, and their prescribed maximum allowable failure probability P_{Fi}^*.

SLSV Method

To improve the computational efficiency, Shan and Wang (2008) developed an effective SLSV method to transform reliability constraints into deterministic constraints (Yang and Gu 2004, 2005; Kogiso et al. 2012; Shan and Wang 2008). The key idea of the SLSV method is that the reliability constraint is transformed to the equivalent deterministic constraint by approximating the MPP using the point obtained from the previous iteration. The SLSV method is briefly introduced herein. For the convenience of discussion, the random variables and random parameters are assumed to obey independent normal distribution. All random variables and random parameters are combined as $\boldsymbol{V} = [\boldsymbol{X}; \boldsymbol{Z}] = [x_1, \ldots, x_m, z_1, \ldots, z_q]^{\mathrm{T}}$, and its mean and deviation vector are $\boldsymbol{\mu} = [\boldsymbol{\mu}_x, \boldsymbol{\mu}_z]^{\mathrm{T}}$ and $\boldsymbol{\sigma} = [\boldsymbol{\sigma}_x, \boldsymbol{\sigma}_z]^{\mathrm{T}}$, respectively. Then the function $P(\cdot)$ in Eq. (1) is defined by

$$P[g_i(\boldsymbol{d}, \boldsymbol{X}, \boldsymbol{Z}) < 0] = P[g_i(\boldsymbol{d}, \boldsymbol{V}) < 0] = \int_{g_i(\boldsymbol{d}, \boldsymbol{V}) < 0} \cdots \int F(\boldsymbol{V}) d\boldsymbol{V} \tag{2}$$

where $F(\cdot)$ = joint probability density function of all random variables. To calculate Eq. (2), the vector $\boldsymbol{V}$ is transformed to the vector $\boldsymbol{U} \in R^{m+q}$ with standard normal distribution

$$u_j = \frac{v_j - \mu_j}{\sigma_j}, \quad j = 1, 2, \ldots, m, m+1, \ldots, m+q \tag{3}$$

where j denotes the jth design parameters which comprises random design variables and random parameters, i.e., $m+q$.

In line with the reference (Ang and Tang 1984), there is

$$\beta_{S_i} = \Phi^{-1}\left[\int_{g_i(\boldsymbol{d}, \boldsymbol{U}) > 0} \cdots \int F(\boldsymbol{U}) d\boldsymbol{U}\right] \approx \frac{-\sum_j u_j^* (\partial g_i / \partial u_j)_*}{\sqrt{\sum_j (\partial g_i / \partial u_j)_*^2}} \tag{4}$$

in which

$$u_j^* = \frac{-(\partial g_i / \partial u_j)_*}{\sqrt{\sum_j (\partial g_i / \partial u_j)_*^2}} \beta_{S_i} \tag{5}$$

where β_{Si} = index of the successful probability of satisfying the ith probabilistic constraint; Φ^{-1} = inverse transformation of

the standard normal distribution; the derivatives $(\partial g_i/\partial u_j)_*$ are evaluated at the MPP $(u_1^*, \ldots, u_{m+q}^*)$; u_j^* = component of $\boldsymbol{U}^*$; and $(\partial g_i/\partial u_j)_*/\sqrt{\sum_j (\partial g_i/\partial u_j)_*^2}$ = direction cosine along the axis u_j.

From Eqs. (5) and (3), there is

$$v_j^* = \mu_j - \beta_{Si}\sigma_j \frac{(\partial g_i/\partial u_j)_*}{\sqrt{\sum_j (\partial g_i/\partial u_j)_*^2}} = \mu_j - \beta_{Si}\sigma_j^2 \frac{(\partial g_i/\partial v_j)_*}{\sqrt{\sum_j [\sigma_j(\partial g_i/\partial v_j)]_*^2}} \quad (6)$$

where * denotes the point in the original design space corresponding to MPP in the normalized variable space, which is also called inverse MPP.

In Eq. (1), the index of desired reliability is rewritten as

$$\beta_{di} = \Phi^{-1}(1 - P_{F_i}^*) \quad (7)$$

and the probabilistic constraint can be expressed by the reliability index

$$\beta_{Si} \geq \beta_{di} \quad (8)$$

To satisfy the reliability requirement, substitute β_{Si} for β_{di} in Eq. (6), there is

$$v_j^* = \mu_j - \beta_{di}\sigma_j^2 \frac{(\partial g_i/\partial v_j)_*}{\sqrt{\sum_j [\sigma_j(\partial g_i/\partial v_j)]_*^2}} \quad (9)$$

During the optimization process, every μ_j has a corresponding inverse MPP v_j^*. Given β_{di} and v_j^* may change on the failure surface as μ_j changes. In addition, μ_j is always located at the origin of the standard normal distribution space. Therefore, assuming that the gradients of the constraint functions g_i ($\boldsymbol{d}$, $\boldsymbol{X}$, $\boldsymbol{Z}$) can be evaluated, one can approximate the direction cosine part, $\sigma_j (\partial g_i/\partial u_j)_*/\sqrt{\sum_j [\sigma_j(\partial g_i/\partial u_j)]_*^2}$ in Eq. (9) by the corresponding mean point μ_j through substituting $(\partial g_i/\partial v_j)_*$ by $(\partial g_i/\partial u_j)$. Thus, there is

$$v_j^* \approx \mu_j - \beta_{di}\sigma_j^2 \frac{\partial g_i/\partial \mu_j}{\sqrt{\sum_j [\sigma_j(\partial g_i/\partial \mu_j)]^2}} \quad (10)$$

Thus, the inverse MPP at $\boldsymbol{V}^*$ at any design point $\boldsymbol{\mu}$ can be directly calculated without the iterative process and double loop. For this method, the derivatives of potential optima $\boldsymbol{\mu}$ are used to approximate the derivatives of inverse MPP $\boldsymbol{V}^*$. So this method is also called mean value-SLSV (MV-SLSV) method. The RBDO based on the SLSV method is simply resolved into a deterministic optimization problem by using the optimization tool.

LSF Method

The aforementioned SLSV method is used to solve the RBDO problem with linear limit-state function by using FORM and thus cannot be applied to high nonlinear problems (Lee et al. 2008). Besides, it is difficult to obtain the derivatives of the limit-state

function of a complex system because the limit-state function is often implicit. To address this issue, the LSF method is proposed by integrating limit-state factors and nominal limit-state functions to transform the reliability constraints to deterministic nominal constraints in this paper. The limit-state function in Eq. (1) is written as

$$P(L|\boldsymbol{d}) = P[g(\boldsymbol{V},\boldsymbol{d}) < 1|\boldsymbol{d}] \le P_F^* \quad \forall\ \boldsymbol{d} \in R^k \tag{11}$$

where $L \equiv [g(\boldsymbol{V},\boldsymbol{d}) \le 1]$ denotes the failure event; $g(\boldsymbol{V},d)$ is called the limit-state function. If a $\eta(d)$ function is found, a positive function called the nominal limit-state function (denoted by nominal function, for short) is

$$P[g(\boldsymbol{V},\boldsymbol{d}) - \eta(\boldsymbol{d})g_n(\boldsymbol{d}) < 0|\boldsymbol{d}] = P_F^* \quad \forall\ \boldsymbol{d} \in R^k \tag{12}$$

The following two constraints are equivalent by Chen et al. 1997:

$$P[g(\boldsymbol{V},\boldsymbol{d}) < 1|\boldsymbol{d}] \le P_F^* \tag{13}$$

and

$$\boldsymbol{\eta}(\boldsymbol{d})g_n(\boldsymbol{d}) \le 1 \tag{14}$$

Therefore, Eq. (12) is rewritten as

$$P\left[\frac{g(\boldsymbol{V},\boldsymbol{d})}{g_n(\boldsymbol{d})} < \eta(\boldsymbol{d})|\boldsymbol{d}\right] = P_F^*, \quad \forall\ \boldsymbol{d} \in R^k \tag{15}$$

In other words, $\eta(\boldsymbol{d})$ is the $(1-P_F^*)$ quantile of the uncertain variable $g(\boldsymbol{V},\boldsymbol{d})/g_n(\boldsymbol{d})$. If the distribution of $g(\boldsymbol{V},\boldsymbol{d})/g_n(\boldsymbol{d})$ is independent of $\boldsymbol{d}$, $\eta(\boldsymbol{d})$ is a constant function. Before the RBDO problem is addressed by adopting the LSF method, the first step is to confirm whether nominal limit-state factor η is a constant.

Define $M \equiv g(\boldsymbol{V},\boldsymbol{d}) - \eta(\boldsymbol{d})g_n(\boldsymbol{d})$, Eq. (12) becomes

$$P(M < 0|\boldsymbol{d}) = P_F^* \quad \forall\ \boldsymbol{d} \in R^k \tag{16}$$

In fact, it is difficult to directly obtain η at a given failure probability. A feasible approach is to achieve a group of samples of (η, P_F^*) by solving Eq. (16), and then to get the nominal limit-state factor at the target probability of failure by using the least-squares method (Naess et al. 2009).

RBDO Thought-Based SLSV-LSF Method

For the high nonlinear and implicit limit-state function in the RBDO problem of the turbine disk, the efficient SLSV-LSF methodology is proposed wherein the deterministic constraints are trans- formed based on the SLSV method or LSF method. If the probabilistic constraint satisfies the requirement of a constant nominal LSF, the LSF method processing the high nonlinear and implicit limit-state function is adopted. Otherwise, the SLSV method decoupling the nested iteration loops is employed to mitigate computational burden and improve computational efficiency. Usually, the procedure to judge η as constant or not is the following: (1) Two feasible turbine disks [for instance, initial design (Model A1) and deterministic optimizer (Model A2)] are chosen. (2) Respective limit-state factors η_1 and η_2 corresponding to Model A1 and Model A2 are determined by performing the probabilistic analysis, i.e., by solving Eq. (16). (3) If the difference between η_1 and η_2 is small enough (i.e., the error $\le 10^{-4}$), the limit-state factor for the reliability constraint M is constant. Therefore, the SLSV- LSF method can improve the computational efficiency and precision due to the superiorities in resolving the high nonlinear and implicit limit-state function, decoupling the nested iteration loops, and transforming uncertainties parameters and constraints into deterministic parameters and constraints. According to the basic idea of the SLSV-LSF method, the flowchart of the RBDO of turbine disk is shown in Fig. 1.

Reliability-Based Design Optimization of Turbine Disk

The turbine disk is a vital component of an aeroengine. Uncertain- ties related to the operating environment, such as rotational speed and structural properties, always result in statistical scatter on turbine disk life (Zhu et al. 2013; Bagaviev and Ulbrich 2004). Therefore, the requirement for cost-effective design has led to the development of probability-based design optimization of the tur- bine disk (Hu and Wang 2008; Hu et al. 2011; Fei et al. 2015b, 2016; Huang et al. 2011). This paper applies the proposed SLSV-LSF method to implement the RBDO of a turbine disk to minimize the mass subjected to the reliability degree. The detailed processes are described in the following steps:

1. Construct the RBDO model: A parametric model is established through the computer-aided design (CAD) package such as *NX UniGraphics* (UG) software. Then a RBDO model for the turbine disk involving design variables, reliability constrains based on the stress criteria, and objective is constructed;

2. Establish surrogate models: A database is established to store the response including constraints and objective for each sampling point, in which sampling points are generated using the design of experiment method. Then the surrogate models for the objective and constraints are constructed using the kriging method;

3. Perform deterministic optimization design: The deterministic optimization design on the turbine disk with the approximated objective and constraints constructed in Step 2 is performed by optimization algorithms. In this step, the deterministic optimizer model is denoted as A2 model;

4. Achieve limit-state factors, that is, reliability analyses on A1 (initial design) and A2 models, respectively, are carried out to determine the corresponding limit-state factors, and to judge as constant or not;

5. Determine transformed deterministic constraints. If the limit- state factors in Step 4 are constant, reliability constraints are transformed into deterministic constraints using LSF method. Otherwise, transformed deterministic constraints are determined by the MV-SLSV method; and

6. Establish RBDO design. Using the same method as in Step 3, obtain the optimizer for the RBDO problem of the turbine disk. Then a convergence test is performed based on the following stopping criterion in Eq. (17):

$$|f(\boldsymbol{d}_i) - f(\boldsymbol{d}_{i-1})| \leq \varepsilon \tag{17}$$

where ε = objective function convergence tolerance supplied by the user; $\boldsymbol{f(d}_i)$ and $\boldsymbol{f(d}_{i\text{-}1})$ = objective functions at design variable $\boldsymbol{d}_i$ for the ith loop; and $d_{i\text{-}1}$ for the (i-1)th loop, respectively. If the convergence test returns true, then the final design is found. Otherwise, the algorithm returns to Step 2 to update the surrogated models and the optimization continues.

Material Preparation

In this paper, the selected turbine disk is manufactured by using a nickel-based superalloy GH4169 in the references (Hu et al. 2011; Hu and Wang 2008). The chemical composition of the alloy includes (in wt%): C 0.07, Cr 20.0, Ni 53.0, Co 0.7, Al 0.5, Mo 3.0, Ti 1.0, Nb 5.1, B 0.01, Mg 0.01, Mn 0.3, Si 0.32, P 0.01, S 0.10, Cu 0.28, Ca 0.02, and the balance Fe. Heat-treatment conditions are (950 – 980)°C±10°C for 60 min, air cooling to 720°C±5°C for 8 h, furnace cooling to 620°C±5°C for 8 h (cooling rate of 50°C/h), and finally air cooling. The tensile properties of the material at room temperature are yield strength 1,181 MPa, ultimate tensile strength 1,374 MPa, and elongation 23%. Tension stress- strain curves under different temperatures are shown in Fig. 2.

Reliability Analysis of Turbine Disk

The meridian plane shape of the turbine disk is shown in Fig. 3 where seven design parameters were selected including baffle thickness (DW2), web outer thickness (DW3), web inner thickness (DW4), bore thickness (DW5), web inner diameter (D_R2), web outer diameter (D_R3), and bore height (DH3).

Periodic modeling was used in this analysis to insure that displacement-constraint equations were automatically imposed on the matched edges of the model. The finite element (FE) model is shown in Fig. 4. Displacement in the axial direction was restricted by a mounting flange. The turbine disk is subjected to a combination of centrifugal loads and thermal loads. Centrifugal forces generated during service were simulated by adding rotational speed on the turbine disk's model. The surface load P_r arising from the rotated turbine blade was imposed on each tooth of the fir-tree slot of the turbine disk, and it was

directly proportional to the rotation-speed square (Zhu et al. 2013). Temperature distribution of the turbine disk is shown in Fig. 5, in which the abscissa axis DIST means radial distance from the bore. The FE model analysis was performed using the commercial package *ANSYS*.

The uncertainties related to the operating environment and material properties will result in scatter of the stresses on the turbine disk. Random variables are shown in Table 1 where random parameters are regarded to be mutually independent.

Based on the stress criteria of the turbine disk referred to as EGD-3 (Ding and Wu 1979), four limit state functions of turbine disk are

$$R_1 = \sigma_{x\_\max}/\sigma_1 \qquad R_2 = \sigma_{y\_\max}/\sigma_2$$
$$R_3 = \sigma_{\bar{y}}/\sigma_3 \qquad R_4 = \sigma_{wy\_\max}/\sigma_4 \tag{18}$$

where $\sigma_{x\_\max}$ = maximum radial stress; $\sigma_{y\_\max}$ = maximum circumferential stress; $\sigma_{\bar{y}}$ = average circumferential stress; and $\sigma_{wy\_\max}$ = maximum circumferential stress on the web region. In this case, these limit state functions in Eq. (18) are nonlinear because the elastic-plastic analysis, as well as contact analysis for the turbine attachment between the turbine disk and the turbine blade, are performed in this study. Thus, failure probabilities of the turbine disk are expressed as follows:

$$P_{F1} = P(\sigma_{x\_\max}/\sigma_1 > 1) \qquad P_{F2} = P(\sigma_{y\_\max}/\sigma_2 > 1)$$
$$P_{F3} = P(\sigma_{\bar{y}}/\sigma_3 > 1) \qquad P_{F4} = P(\sigma_{wy\_\max}/\sigma_4 > 1) \tag{19}$$

The nominal limit-state function of R_1 is chosen as $R_{n1} = R_1[E(\boldsymbol{V}), \boldsymbol{d}]$. Then, the following is defined:

$$M_1 \equiv R_1/R_{n1} - \eta_1 = \sigma_{x\_\max}/(\tilde{\sigma}_{x\_\max} * s) - \eta_1 \tag{20}$$

where $\sigma\sim$ = maximum radial stress of turbine disk when the values of random variables $\boldsymbol{V}$ are equal to their mean value, $s = \sigma_1/\sigma\sim 1$; $\sigma\sim 1$ = mean value of σ_1. Thus, $s \sim N(1; 0.1^2)$. Similarly, M_2, M_3, and M_4 are

$$M_1 = R_1/R_{n1} - \eta_1 = \sigma_{x\_\max}/(\tilde{\sigma}_{x\_\max} * s) - \eta_1$$
$$M_2 = R_2/R_{n2} - \eta_2 = \sigma_{y\_\max}/(\tilde{\sigma}_{y\_\max} * s) - \eta_2$$
$$M_3 = R_3/R_{n3} - \eta_3 = \sigma_{\bar{y}}/(\tilde{\sigma}_{\bar{y}} * s) - \eta_3$$
$$M_4 = R_4/R_{n4} - \eta_4 = \sigma_{wy\_\max}/(\tilde{\sigma}_{wy\_\max} * s) - \eta_4 \tag{21}$$

Then the number of random variables in Table 1 is reduced to 4, namely, $\boldsymbol{V}(n, \rho, P_r, s)$. Based on limit-state factor method in the previous section, two feasible turbine disks (Model A1 and Model A2) are chosen to confirm whether nominal limit-state factors are constant, in which feasible A1 and A2 models are arbitrary as long as their design parameters are within the ranges from lower bound to upper bound. The detailed structural parameters for A1 and A2 are listed in Table 2, and the stress distributions on the A1 and A2 models are shown in Fig. 6. By using the combination of response surface method and Monte Carlo simulation method with 10^6 samplings, limit-state factors at different failure probabilities are shown in Table 3.

From Table 3 it is demonstrated that (1) large error of limit-state factors appears at low failure probabilities and (2) the error of limit- state factor for $M3$ is the minimum because the order of magnitude is 10^{-4}. Considering the error from the Monte Carlo simulation, one may think the limit-state factor η_3 of $M3$ is constant.

Sensitivity analyses of $R_i (i = 1, \ldots, 4)$ were adopted to determine main random variables. Sensitivity analysis results are shown in Fig. 7. It is revealed that material density plays the least role in the stress constraint index. Thus, material density can be treated as deterministic parameter during reliability analysis on turbine disk.

Reliability Optimization of Turbine Disk

Considering failure probability of permissible maximum radial stress and average circumferential stress as uncertain

constraints, one can construct the RBDO problem of the turbine disk, which minimizes disk mass subject to uncertain constraints. The RBDO problem of turbine disk is formulated as

$$\begin{aligned}
&\min \text{volume} = f(\text{DW2}, \text{DW3}, \text{DW4}, \text{DW5}, \text{DH3}, \text{D_R2}, \text{D_R3}) \\
&\text{s.t. } P_i(R_i > 1) \le 0.13\% \quad (i = 1, 2, 3, 4) \\
&R_1 \le 1, R_2 \le 1, R_3 \le 1, R_4 \le 1 \qquad 16.0 \le \text{DW2} \le 24.0, \\
&12.0 \le \text{DW3} \le 18.0 \qquad 15.0 \le \text{DW4} \le 19.0, \quad 45.0 \le \text{DW5} \le 60.0 \\
&25.0 \le \text{DH3} \le 40.0, \quad 180.0 \le \text{D_R2} \le 210.0 \\
&210.0 \le \text{D_R3} \le 235.0
\end{aligned} \tag{22}$$

where design variable vector $\boldsymbol{d}$ = {DW2; DW3; DW4; DW5; DH3; D_R2; D_R3}; random variable $\boldsymbol{V}$ = {n, P_r, s}. Then based on reliability analysis of turbine disk in the previous section, limit-state factor η_3 = 1.482 and Eq. (22) is rewritten as

$$\begin{aligned}
&\min \text{volume} = f(\text{DW2}, \text{DW3}, \text{DW4}, \text{DW5}, \text{DH3}, \text{D_R2}, \text{D_R3}) \\
&\text{s.t. } P_i(R_i > 1) \le 0.13\% \quad (i = 1, 2, 4) \\
&R_1 \le 1, R_2 \le 1, 1.482Rn_3 \le 1, R_4 \le 1 \qquad 16.0 \le \text{DW2} \le 24.0, \\
&12.0 \le \text{DW3} \le 18.0 \qquad 15.0 \le \text{DW4} \le 19.0, \quad 45.0 \le \text{DW5} \le 60.0 \\
&25.0 \le \text{DH3} \le 40.0, \quad 180.0 \le \text{D_R2} \le 210.0 \\
&210.0 \le \text{D_R3} \le 235.0
\end{aligned} \tag{23}$$

After transforming uncertain constraint R_3 into deterministic constraint based on LSF method, Eq. (23) was solved by applying reliability-based design optimization methods with kriging surrogate model to reduce the total number of expensive function evaluations (Basudhar et al. 2008). By the proposed SLSV-LSF method, the RBDO of the turbine disk was completed. The optimization results were compared with those of PMA method, SLSV method, and LSF method as shown in Table 4. Major findings of this study can be summarized as follows:

- By comparing against the deterministic optimization, the design variables in the RBDO problem of the turbine disk including DW3 and DW4 increased in order to satisfy the reliability con- straint of the maximum radial stress;
- For computational precision, the RBDO result of the SLSV-LSF method is close to that of the PMA approach, which indicates that the proposed SLSV-LSF method pledges the accuracy of the RBDO of turbine disk;
- For computational efficiency, the numbers of function evaluation (FE analysis) and iterations required for the proposed SLSV-LSF method is equal to these of deterministic optimization design and almost close to optimization results with 50% reliability in the reference Hu et al. (2011), which is far less than that from PMA method. The iterations of the SLSV-LSF method is basically one-third the PMA method. The number of function evaluation of the SLSV-LSF method is nearly one-third the PMA method. Therefore, the SLSV-LSF method is demonstrated to hold high computational efficiency; and
- The SLSV cannot implement the RBDO of turbine disk with a large number of high nonlinear and implicit limit-state functions because the methodology is poor at dealing with the nonlinear and implicit limit-state functions.

In conclusion, the optimization results in this study agree well with those of traditional RBDO methods (PMA, for instance). However, the computational cost of interest decreases dramatically since the reliability constraints are transformed into deterministic constraints, which verifies the proposed SLSV-LSF method has higher computational efficiency.

Conclusions

In this study, the SLSV-LSF approach of transforming uncertain constraints into deterministic constraints was presented by synthetically using the superiorities of the SLSV method and the LSF method to improve the computational efficiency of turbine disk RBDO. Through this study, some conclusions are summarized as follows:

- From the reliability analysis of the turbine disk, it is reasonable that the limit-state factor of uncertain average

circumferential stress constraint is regarded to be constant. Besides, material density is insignificant and thus may be treated as a deterministic parameter;

- As demonstrated from the RBDO of a turbine disk, the proposed SLSV-LSF method is promising to resolve the nonlinear and implicit limit-state functions in RBDO and decouple the nested iterations loop problem into a single-loop problem, so that the proposed method features low computational cost and high de- sign efficiency while maintaining the computing precision; and
- The efforts provide a promising approach for the RBDO of com- plex structure.

Acknowledgments

The paper is cosupported by the National Natural Science Foundations of China (Grant Nos. 51305012 and 51375031), Aviation Science Fund of China (Grant No. 2014ZB51), Defense Industrial Technology Development Program (Grant No. B2120132006), General Research Grant from Hong Kong SAR Government [Grant No. 514013(B-Q39B)], the funding of Hong Kong Scholars Programs (Grant Nos. XJ2015002 and G-YZ90), and China's Postdoctoral Science Funding (Grant No. 2015M580037). The authors would like to thank them.

Notation

The following symbols are used in this paper:

$c(\cdot)$ = deterministic constraint function;

$\boldsymbol{d}$ = vector of deterministic design variables;

$F(\cdot)$ = probability density function;

$f(\cdot)$ = objective function;

$g(\cdot)$ = limit-state function;

i, j = ith, jth calculation in RBDO design;

k = number of deterministic design variables;

L = failure event;

m = number of random design variables;

n = number of probabilistic constraints;

$P(\cdot)$ = probability function;

P_F^*= maximum allowable failure probability;

q = number of random parameters;

R = real number space;

t = number of deterministic constraints;

$\boldsymbol{U}$ = transformed vector of V with standard normal distribution;

$\boldsymbol{V}$ = combining vector of random design variables and random design parameters;

$\boldsymbol{X}$ = vector of random design variables;

x = element in X;

$\boldsymbol{Z}$ = vector of random parameters;

z = element in Z;

β = index of reliability;

δ = deviation vector;

μ = mean vector;

Φ^{-1} = inverse transformation of the standard normal distribution;

∂= partial derivative; and

* = inverse most probable point.

References

Ang, A. H. S., and Tang, W. H. S. (1984). *Probability concepts in engineering planning and design*, Wiley, New York.

ANSYS 14.0 [Computer software]. ANSYS, Canonsburg, PA.

Bagaviev, A., and Ulbrich, A. (2004). "Life assessment of turbine compo- nents based on deterministic and probabilistic procedures." *Int. J. Pressure Vessels Piping*, 81(10-11), 855–859.

Basha, B. M., and Babu, G. L. S. (2010). "Reliability assessment of internal stability of reinforced soil structures: A pseudo-dynamic approach." *Soil Dyn. Earthquake Eng.*, 30(5), 336–353.

Basha, B. M., and Babu, G. L. S. (2011). "Reliability based earthquake resistant design for internal stability of reinforced soil structures." *Geotech. Geol. Eng.*, 29(5), 803–820.

Basudhar, A., Missoum, S., and Sanchez, A. H. (2008). "Limit state function identification using support vector machines for discontinuous responses and disjoint failure domains." *Probab. Eng. Mech.*, 23(1), 1–11.

Chen, X., Hasselman, T. K., and Neill, D. J. (1997). "Reliability based structural design optimization for practical applications." *38th AIAA/ASME/ASCE/AHS/ASC Structures, Structural Dynamics, and Materials Conf.*, AIAA, Reston, VA.

Ching, J., and Hsu, W. C. (2008a). "Transforming reliability limit-state constraints into deterministic limit-state constraints." *Struct. Saf.*, 30(1), 11–33.

Ching, J. Y., and Hsu, W. C. (2008b). "Approximate optimization of systems with high-dimensional uncertainties and multiple reliability constraints." *Comput. Methods Appl. Mech. Eng.*, 198(1), 52–71.

Ching, J. Y., and Hsu, W. C. (2008c). "Transforming reliability limit-state constraints into deterministic limit-state constraints." *Struct. Saf.*, 30(1), 11–33.

Chiralaksanakul, A., and Mahadavan, S. (2005). "First-order approximation methods in reliability-based design optimization." *J. Mech. Des.*, 127(5), 851–857.

Ding, A. X., and Wu, J. (1979). "Spey MK202 engine stress criteria (EGD-3)." International Aviation Editorial Dept., Beijing.

Doltsinis, I., and Kang, Z. (2004). "Robust design of structures using optimization methods." *Comput. Methods Appl. Mech. Eng.*, 193(23-26), 2221–2237.

Elms, D. G. (2004). "Structural safety—issues and progress." *Prog. Struct. Eng. Mater.*, 6(2), 116–126.

Fei, C. W., Bai, G. C., Tang, W. Z., and Choy, Y. (2015a). "Optimum control for nonlinear dynamic reliability radial deformation of turbine casing with T-LSSVM." *Adv. Mater. Sci. Eng.*, 2015, 680406.

Fei, C. W., Bai, G. C., Tang, W. Z., Choy, Y. S., and Gao, H. F. (2016). "Transient reliability optimization for turbine disk radial deformation." *J. Central South Univ.*, 23(2), 344–352.

Fei, C. W., Tang, W. Z., and Bai, G. C. (2014a). "Novel method and model for dynamic reliability optimal design of turbine blade." *Aerosp. Sci. Technol.*, 39(6), 588–595.

Fei, C. W., Tang, W. Z., and Bai, G. C. (2014b). "Study on the theory, method and model for mechanical dynamic assembly reliability optimization." *Proc. IME Part C-J. Mech. Eng. Sci.*, 228(16), 3019–3038.

Fei, C. W., Tang, W. Z., and Bai, G. C. (2015b). "Nonlinear dynamic probabilistic design of turbine disk-radial deformation using extremum response surface method-based support vector machine of regression." *Proc. IME Part G-J. Mech. Eng. Sci.*, 229(2), 290–300.

Hu, D. Y., and Wang, R. Q. (2008). "Probabilistic analysis on turbine disk under LCF-creep." *Proc., ASME Turbo Expo 2008: Power for land, Sea, and Air*, The American Society of Mechanical Engineers, New York, NY.

Hu, D. Y., Wang, R. Q., and Tao, Z. (2011). "Probabilistic design for turbine disk at high temperature." *Aircraft Eng. Aerosp. Technol.*, 83(4), 199–207.

Huang, M. F., Chan, C. M., and Lou, W. J. (2012). "Optimal performance- based design of wind sensitive tall buildings considering

uncertainties.” *Comput. Struct.*, 98-99, 7–16.

Huang, Z. H., Wang, C. E., Chen, J., and Tian, H. (2011). “Optimal design of aeroengine turbine disk based on Kriging surrogate models.” *Comput. Struct.*, 89(1-2), 27–37.

Kogiso, N., Yang, Y. S., Kim, Y. S., and Lee, J. O. (2012). “Modified single-loop-single-vector method for efficient reliability-based design optimization.” *J. Adv. Mech. Des. Syst. Manuf.*, 6(7), 1206–1220.

Kokkolaras, M., Mourelatos, Z. P., and Papalambros, P. Y. (2006). “Impact of uncertainty quantification on design: An engine optimization case study.” *Int. J. Reliab. Saf.*, 1(1-2), 225–237.

Lee, I., Choi, K. K., Du, L., and Gorsich, D. (2008). “Inverse analysis method using MPP-based dimension reduction for reliability-based design optimization of nonlinear and multi-dimensional systems.” *Comput. Methods Appl. Mech. Eng.*, 198(1), 14–27.

Liang, J. H., Mourelatos, Z. P., and Nikolaidis, E. (2007). “A single-loop approach for system reliability-based design optimization.” *J. Mech. Des.*, 129(12), 1215–1224.

Liu, P., and Der Kiureghian, A. (1991). “Optimization algorithms for struc- tural reliability.” *Struct. Saf.*, 9(3), 161–177.

Mishra, S. K., Roy, B. K., and Chakraborty, S. (2013). “Reliability-based- design-optimization of base isolated buildings considering stochastic system parameters subjected to random earthquakes.” *Int. J. Mech. Sci.*, 75(9), 123–133.

Naess, A., Leira, B. J., and Batsevych, O. (2009). “System reliability analysis by enhanced Monte Carlo simulation.” *Struct. Saf.*, 31(5), 349–355.

NX Unigraphics 7.5 [Computer software]. Siemens PLM Software, Plano, TX.

Papadrakakis, M., Lagaros, N. D., and Plevris, V. (2005). “Design optimi- zation of steel structures considering uncertainties.” *Eng. Struct.*, 27(9), 1408–1418.

Shan, S. Q., and Wang, G. G. (2008). “Reliable design space and complete single-loop reliability-based design optimization.” *Reliab. Eng. Syst. Saf.*, 93(8), 1218–1230.

Spence, S. M. J., and Gioffre, M. (2011). “Efficient algorithms for the reliability optimization of tall buildings.” *J. Wind Eng. Ind. Aerodyn.*, 99(6–7), 691–699.

Tu, J., and Choi, K. K. (1999). “A new study on reliability-based design optimization.” *J. Mech. Des.*, 121(4), 557–564.

Wu, Y. T., Shin, Y., Sues, R. H., and Cesare, M. A. (2001). “Safety-factor based approach for probabilistic-based design optimization.” *42nd AIAA/ASME/ASCE/AHS/ASC Structures, Structural Dynamics, and Materials Conf.*, AIAA, Reston, VA.

Yang, R. J., and Gu, L. (2004). “Experience with approximate reliability- based optimization methods.” *Struct. Multidiscipl. Optimiz.*, 26(1-2), 152–159.

Yang, R. J., and Gu, L. (2005). “Experience with approximate reliability- based optimization methods II: An exhaust system problem.” *Struct. Multidiscipl. Optimiz.*, 29(6), 488–497.

Yao, W., Chen, X., Luo, W., Tooren, M. V., and Guo, J. (2011). “Review of uncertainty-based multidisciplinary design optimization methods for aerospace vehicles.” *Prog. Aerosp. Sci.*, 47(6), 450–479.

Zhu, S. P., Huang, H. Z., Smith, R., Ontiveros, V., He, L. P., and Modarres,

M. (2013). “Bayesian framework for probabilistic low cycle fatigue life prediction and uncertainty modeling of aircraft turbine disk alloys.” *Probab. Eng. Mech.*, 34(1), 114–122.

Figures

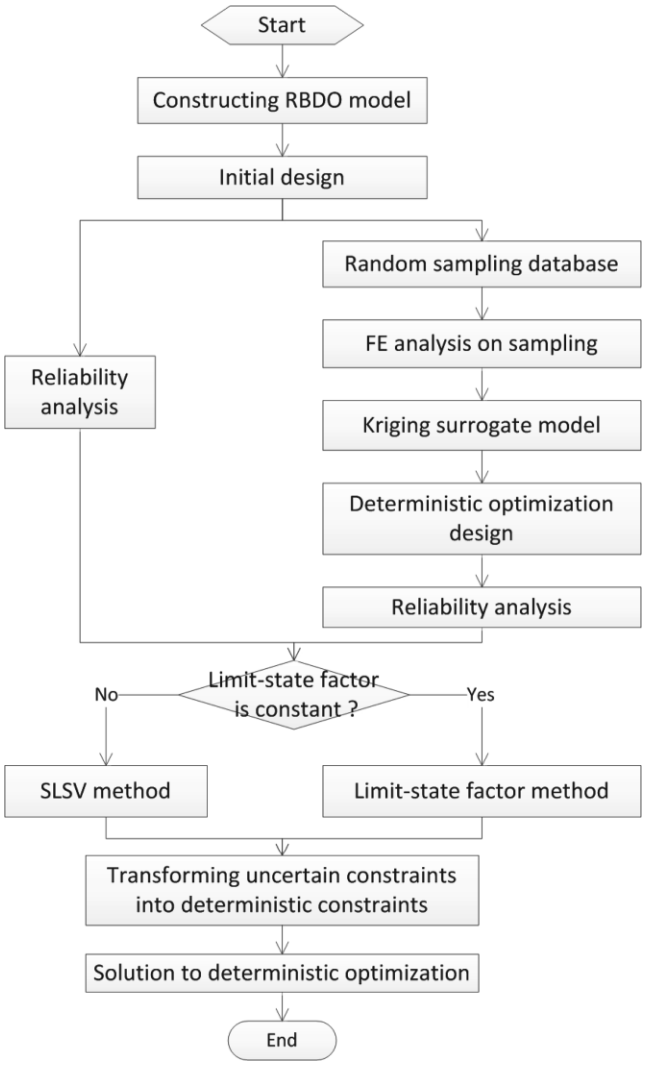

Fig. 1. Flowchart of RBDO of the turbine disk

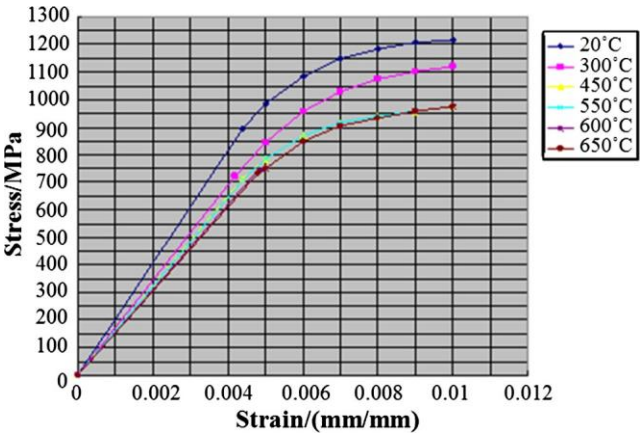

Fig. 2. Stress-strain curves of GH4169 superalloy

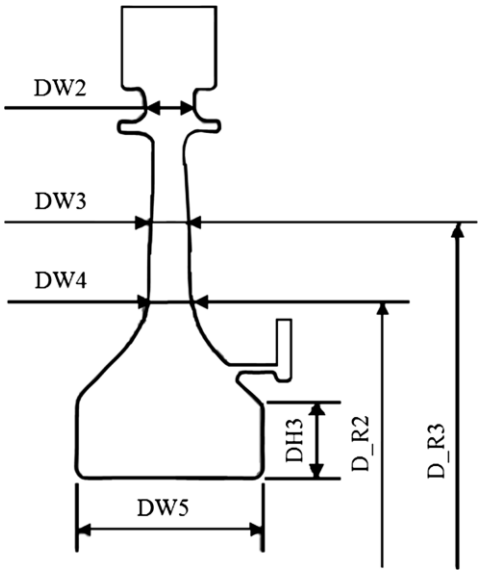

Fig. 3. Turbine disk drawing

Fig. 4. FE model of turbine disk

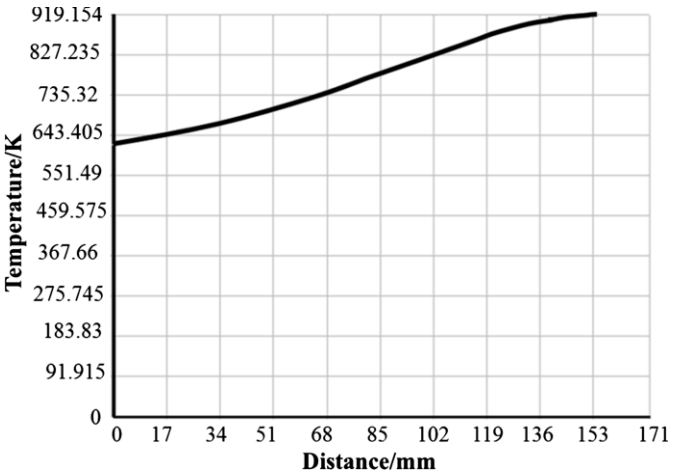

Fig. 5. Temperature distribution (K) of turbine disk along radial direction

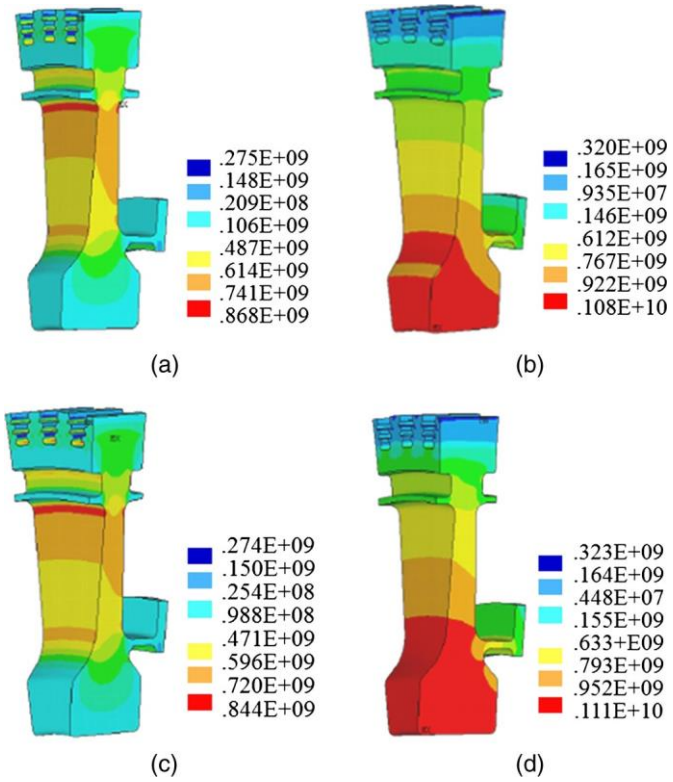

Fig. 6. Stress distribution (Pa) of A1 and A2 models: (a) radial stress distribution (Pa) of A1 model; (b) circumferential stress distribution (Pa) of A1 model; (c) radial stress distribution (Pa) of A2 model; (d) circumferential stress distribution (Pa) of A2 model

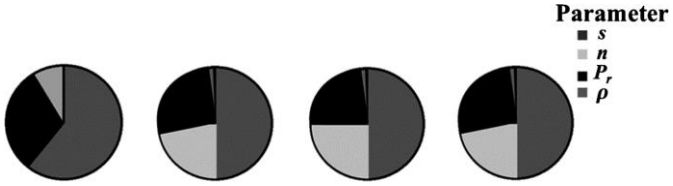

Fig. 7. Sensitivity analysis results of random variables

Tables

Random variable	Mean value	Coefficient of variation (COV)	Distributions
Rotational speed n, rad/s	1,078.6	0.05	Normal
Material density ρ, kg/m^3	8,240	0.005	Normal
Surface load P_r, 10^6 Pa	385.6	0.10	Normal
Maximum permissible radial stress σ_1, 10^6 Pa	1,003.3	0.10	Normal
Maximum permissible circumferential stress σ_2, 10^6 Pa	1,043.6	0.10	Normal
Maximum permissible average circumferential stress σ_3, 10^6 Pa	1,017.9	0.10	Normal
Maximum permissible circumferential stress at the web region σ_4, 10^6 Pa	1,003.3	0.10	Normal

Table 1. Statistics of Random Variables

Parameters	A1 (initial design)	A2 (feasible model)	Lower bound	Upper bound
DW2, 10^{-3} m	19.60	21.38	16.00	24.00
DW3, 10^{-3} m	14.50	13.63	12.00	18.00
DW4, 10^{-3} m	17.00	15.00	15.00	19.00
DW5, 10^{-3} m	52.00	51.49	45.00	60.00
DH3, 10^{-3} m	30.00	25.00	25.00	40.00
D_R2, 10^{-3} m	195.00	180.00	180.00	210.00
D_R3, 10^{-3} m	225.00	210.00	210.00	235.00
σ_{x_max}, 10^6 Pa	838.67	849.26	—	1,003.3
σ_{y_max}, 10^6 Pa	1,068.6	996.88	—	1,043.6
σ_y, 10^6 Pa	640.91	719.15	—	1,017.9
σ_{wy_max}, 10^6 Pa	978.19	809.04	—	1,003.3
Volume, 10^{-4} m^3	1.491	1.382	—	—

Table 2. Structural Parameters of Turbine Disk

	M_1			M_2			M_3			M_4		
P_F, %	A1	A2	Error, 10^{-3}	A1	A2	Error, 10^{-3}	A1	A2	Error, 10^{-3}	A1	A2	Error, 10^{-3}
50	0.994177	0.99109	3.087	0.995607	0.993362	2.245	1.00098	1.00087	0.11	1.0005	0.997193	3.31
10	1.15929	1.15568	3.61	1.16911	1.15937	9.74	1.18074	1.18052	0.22	1.17592	1.16952	6.40
5.0	1.21315	1.20863	4.52	1.22516	1.21362	11.54	1.23903	1.23876	0.27	1.23234	1.22504	7.30
2.0	1.27728	1.27167	5.61	1.29145	1.27804	13.41	1.30708	1.30678	0.30	1.29832	1.29025	8.07
1.0	1.32224	1.31519	7.05	1.3377	1.32323	14.47	1.35573	1.35533	0.40	1.34524	1.33663	8.61
0.2	1.41596	1.40741	8.55	1.43434	1.41745	16.48	1.45572	1.45521	0.51	1.44174	1.4318	9.94
0.13	1.4409	1.43143	9.47	1.45868	1.44302	15.66	1.4819	1.48157	0.33	1.46646	1.45692	9.54

Table 3. Limit-State Factors under Different Failure Probabilities

Parameters	Initial design	Deterministic optimization	RBDO results	
			PMA	SLSV-LSF
Objective				
Volume, 10^{-4} m^3	1.491	1.475	1.524	1.525
Design variables				
DW2, 10^{-3} m	19.60	24.60	16.00	16.00
DW3, 10^{-3} m	14.50	10.875	16.10	16.21
DW4, 10^{-3} m	17.00	12.75	18.00	18.00
DW5, 10^{-3} m	52.00	65.00	65.00	65.00
DH3, 10^{-3} m	30.00	22.50	20.00	20.00
D_R2, 10^{-3} m	195.00	180.00	180.00	180.00
D_R3, 10^{-3} m	225.00	235.00	235.00	235.00
Constraints				
σ_{x_max}, 10^6 Pa	838.67	969.33	724.64	730.69
σ_{y_max}, 10^6 Pa	1,068.6	1,025.1	1,035.75	1,035.9
σ_y, 10^6 Pa	640.91	628.38	613.16	612.94
σ_{wy_max}, 10^6 Pa	978.19	907.33	941.73	941.12
Iterations	—	5	14	5
Function evaluation	—	35	102	35

Table 4. Comparison of Optimization Results